

GLOBAL MAPPING OF NEAR-SURFACE WATER-EQUIVALENT HYDROGEN. Asmin V. Pathare¹, William C. Feldman¹, Thomas H. Prettyman¹, Elizabeth Jensen¹, and Sylvestre Maurice², ¹Planetary Science Institute, Tucson, AZ 85719 (pathare@psi.edu), ²IRAP, Université Paul Sabatier, CNRS, Toulouse, France.

Introduction: We report on MDAP-funded efforts to improve upon global mapping of near-surface water-equivalent hydrogen (WEH). To date, more than 3.5 Mars years of neutron data measured by the Mars Odyssey Neutron Spectrometer (MONS) have been analyzed to develop global maps of hydrogen concentration interpreted using a simple 2D model of the outer ~0.5 meter of Martian crust [1]. A two-layer near-surface regolith model is assumed that expresses hydrogen concentration in terms of: (1) an upper layer of weight fraction W_{up} having (2) thickness D overlying a (3) semi-infinite lower layer of weight fraction W_{dn} .

Initial MONS-derived global maps of W_{dn} and D assumed constant W_{up} [2]. More recently, *Feldman et al.* [3] self-consistently calculated W_{up} directly from MONS data using “cross over” of fast vs. epithermal neutrons with unity line for large representative regions of interest (ROIs). However, application of this crossover technique using unweighted sliding 1800-km diameter ROIs resulted in large areas at low latitudes with unphysical negative values of W_{up} [3]. Here, we recompute W_{up} using distance-weighted ROIs and linear chi-squared minimization regression (Fig. 2), resulting in just one unphysical negative region (in Valles Marineris). **Figure 2 thus represents the best mid-latitude map of W_{up} to date** (note values poleward of 60° will likely require a quadratic instead of linear fit).

For known crossovers, values of W_{dn} and D can more accurately be determined via 3D interpolation (Fig. 1) of W_{up} -dependent simulated grids of thermal and epithermal MONS counts along W_{dn} and D contours (not shown). For example, the “Old” method of MONS mapping of W_{dn} [1] in the vicinity of five recent ice-rich mid-latitude craters (Fig. 3) identified by *Byrne et al.* [4] yields values of “Old Wdn” at four impact sites much lower than the 26% threshold for excess ice (Table 1). This is problematic, as the relatively rapid sublimation of exposed ice in the craters implies the presence of discrete clean ice at fractions well above that of the 26 wt% pore ice maximum [4,5]. Our “New” method of crossover-dependent MONS mapping, however, results in much higher values of W_{dn} (51%-96%) that are consistent with the presence of excess ice at all five recent impact sites (Table 1).

Further Work: We will also improve spatial crossover resolution by deconvolving the intrinsic spatial resolution of the MONS sensors. We have recently successfully applied an improved spatial deconvolution algorithm to most of the MONS Prism 1 (downward-facing) sensor data, from which we derive epithermal

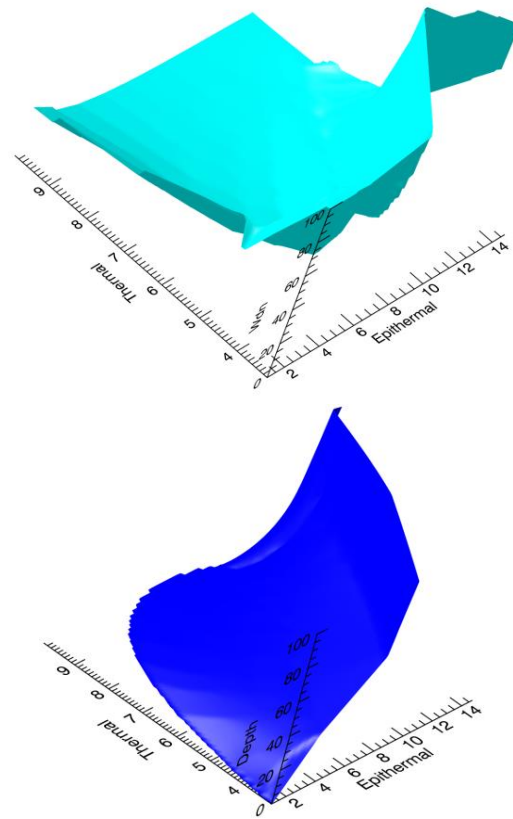


Figure 1: 3D plots of W_{dn} (top) and burial depth D (bottom) interpolated from irregular grid for “S21” soil composition [6] and $W_{up} = 1\%$. Additional W_{dn} and D plots also generated for $W_{up} = 2/3/4\%$ (not shown).

neutron fluxes. This will significantly improve the resolution of the epithermal neutron counting rates needed for determination of W_{up} by up to a factor of 2. Subsequent deconvolution of Prism 2 (forward-facing) and Prism 4 (backward-facing) will likewise improve the resolution of the thermal neutron mapping needed for definition of W_{dn} and D once our revised global mapping of W_{up} is completed. Ultimately, our objective is to continue the progress made with weighted fitting, 3D interpolation, and spatial deconvolution techniques that include fast and thermal neutron counting rates to produce more accurate W_{up} -dependent global maps of W_{dn} and D at higher spatial resolution.

References: [1] Maurice S. et al. (2011) *JGR*, 116, E11008. [2] Feldman W.C. et al. (2004) *JGR*, 109, E09006. [3] Feldman W.C. et al. (2011) *JGR*, 116, E11009. [4] Byrne S. et al. (2009) *Science*, 325, 1674-1676. [5] Dundas C.M. et al. (2014) *JGR*, 119, 109-127. [6] Diez B. et al. (2008) *Icarus*, 196, 409-421. [7] Mellon M.T. et al. (2004) *Icarus*, 169, 324-340.

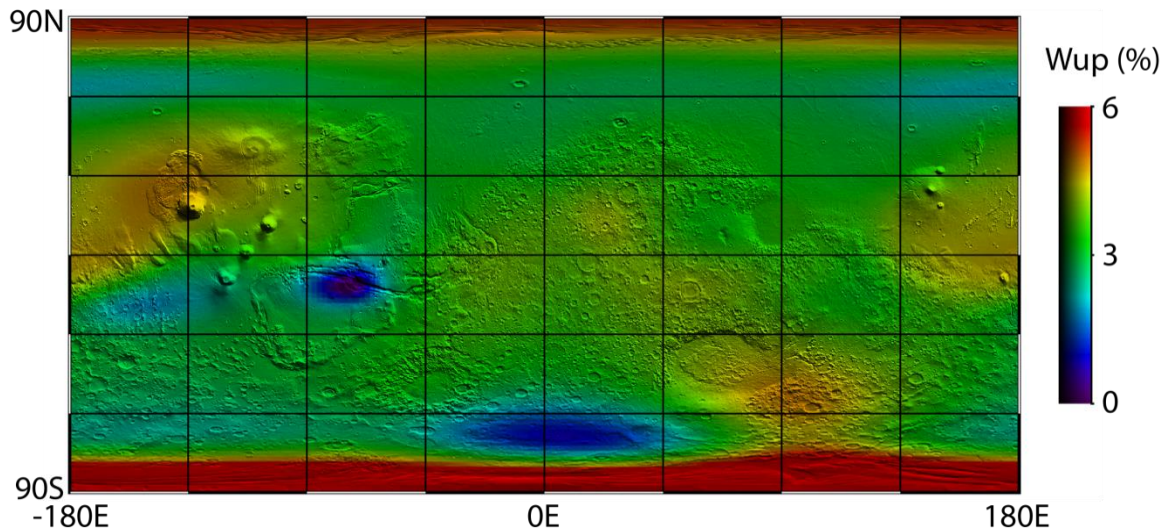


Figure 2: Map of W_{up} = crossover points from the linear chi-squared minimization regressions between WEHD0(fast) and WEHD0(epi) data in inverse distance-squared weighted regions of interest spaced every two degrees of latitude and longitude. The dynamic range spans 0-6, so the purple (in Valles Marineris) actually corresponds to unphysical negative values, and the red to highly positive values.

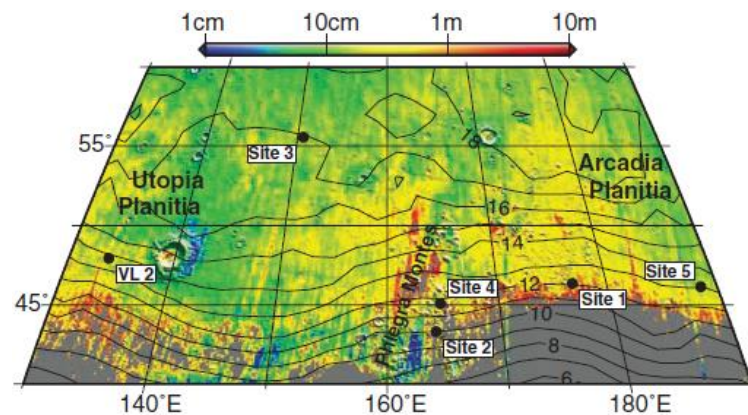


Figure 3: Taken from *Byrne et al.* [4]. Locations of five recent ice-rich impacts (“Site 1-5”) and Viking Lander 2 (“VL2”). Color bar represents expected ice depths modeled by *Mellon et al.* [7]. Contours are MONS-derived burial depths (g/cm^2) from *Feldman et al.* [2].

Crater	Lat (N)	Long (E)	Old W_{up} (%)	New W_{up} (%)	Old W_{dn} (%)	New W_{dn} (%)	Old D (g/cm^2)	New D (g/cm^2)	Model D (g/cm^2)
Site 1	46.33°	176.90°	4.35	2.85	10.0	86.6	19.4	52.8	34
Site 2	43.28°	164.22°	4.35	2.87	9.3	68.6	16.5	48.9	49
Site 3	55.57°	150.62°	4.35	1.18	28.0	50.7	22.7	31.2	8
Site 4	45.05°	164.71°	4.35	2.70	9.8	66.1	17.8	46.9	25
Site 5	46.16°	188.51°	4.35	3.17	14.2	95.9	19.0	50.0	9

Table 1: Adapted from *Byrne et al.* [4]. “Old” [3] and “New” (this abstract) MONS-derived values of W_{up} , W_{dn} , and D at five recent impact sites shown in Fig. 3. The short-lived presence of ice [4] implies discrete layer of excess ice greater than pore space limit ($W_{dn} = 26$ wt%) that is predicted at each site by “New” (but not “Old”) MONS methodology. The “New” MONS-derived D values are also a somewhat better fit to ice depths modeled by *Mellon et al.* [7] assuming a nominal soil density of $1.5 \text{ g}/\text{cm}^3$.